

26 ***GISAXS Critical Angle***

27 Our GISAXS measurements were conducted at water-substrate interfaces. Here, we have
28 used Snell Equation (Eqn. (1)) to calculate the critical angle (α_1) for total external X-ray
29 reflection.¹

$$30 \alpha_1 = \arccos \left(\frac{1 - \delta_{\text{substrate}}}{1 - \delta_{\text{water}}} \right) \left(\frac{180}{\pi} \right) \quad (1)$$

31 Where, $\delta_{\text{substrate}}$ and δ_{water} represent the refraction indices of the substrates and water,
32 respectively. With density values of 2.68, 3.97, and 1.00 g/cm³ for SiO₂, Al₂O₃, and H₂O and an
33 X-ray energy of 14 KeV, the indices of refraction (δ) for SiO₂, Al₂O₃, and H₂O were calculated
34 to be 2.85×10^{-6} , 4.14×10^{-6} , and 1.18×10^{-6} , respectively.¹ Applying Eqn. (1), the critical
35 angles for total external X-ray reflection at water-SiO₂ and water-Al₂O₃ interfaces were
36 calculated to be 0.105° and 0.136°, respectively. Therefore, 0.10° was chosen as the incident
37 angle for all sample measurements.

38 ***XPS Measurements***

39 X-ray photoelectron spectroscopy (XPS) measurements were also conducted to determine
40 the oxidation states of Mn in the precipitates formed from FeMn solution. To collect enough
41 precipitates, 500 mL FeMn solution (Table 1) was freshly prepared and let to sit for 1 hr. Then,
42 the particles were collected using centrifugal filter unit, and were transferred to a gold wafer.
43 After drying the sample in a desiccator overnight, the photo-electrons, produced via a
44 monochromatic Al-k X-ray source (1486.6 eV) operated at 350 W, were collected on a Physical
45 Electronics Model 5700 X-ray photoelectron spectroscopy (XPS) instrument. The analyzed area,
46 collection solid cone and take off angle were set at 800 m, 5° and 45°, respectively. All spectra

47 were acquired under vacuum condition ($< 5 \times 10^{-9}$ torr). Data processing was carried out using
48 the Multipak™ software package. A Shirley background subtraction was applied. Unfortunately,
49 the amounts of Mn in Mn-bearing ferrihydrite nanoparticles on substrates were lower than the
50 detection limits of XPS measurements (Figure S2).

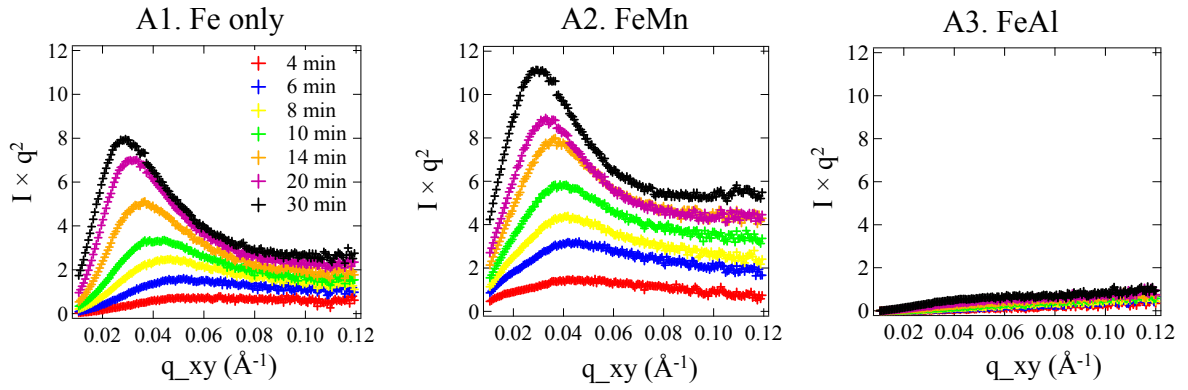
51 *Mn²⁺ and Al³⁺ ion adsorption vs. Mn(OH)₂ and Al(OH)₃ precipitation on substrates*

52 The zeta potential changes of the substrates in Mn and Al solutions could be caused by
53 either Mn²⁺ and Al³⁺ ion adsorption or heterogeneous precipitation of Mn(OH)₂ and Al(OH)₃ on
54 substrates. In our previous study, GISAXS control experiment with 0.5 mM Al(NO₃)₃ solution in
55 contact with quartz under similar experimental condition (0.5 mM Al(NO₃)₃ and pH = 3.7 ± 0.1)
56 was conducted. No GISAXS scattering curves were measured after background subtraction,
57 indicating no Al(OH)₃ particle formation on quartz.² Accordingly, in this study, the formation of
58 Al(OH)₃ particles on substrates was not expected as well. Meanwhile, at 25 °C, the solubility of
59 Al(OH)₃ ($K_{sp} = 1.3 \times 10^{-33}$) is much lower than Mn(OH)₂ ($K_{sp} = 1.9 \times 10^{-13}$). Therefore, the
60 solutions were slightly undersaturated with respect to Al(OH)₃ (saturation index = - 0.08) and
61 highly undersaturated with respect to Mn(OH)₂ (saturation index = -10.8). That means, if the
62 formation of Al(OH)₃ on substrates did not occur, the formation of Mn(OH)₂ on substrates
63 should not be expected as well. Therefore, Mn²⁺ and Al³⁺ ion adsorption rather than
64 heterogeneous precipitation of Mn(OH)₂ and Al(OH)₃ on substrates were likely to have occurred,
65 which changed the zeta potential values of substrates.

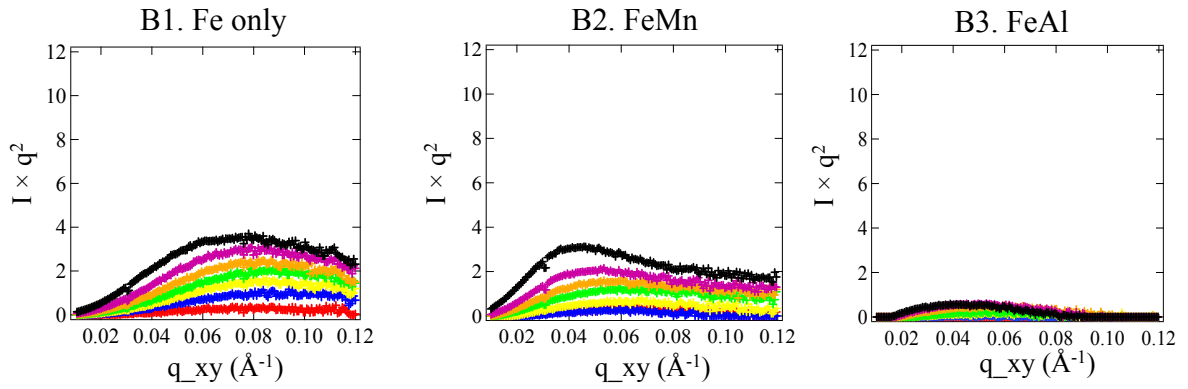
66

67

Particles on Quartz



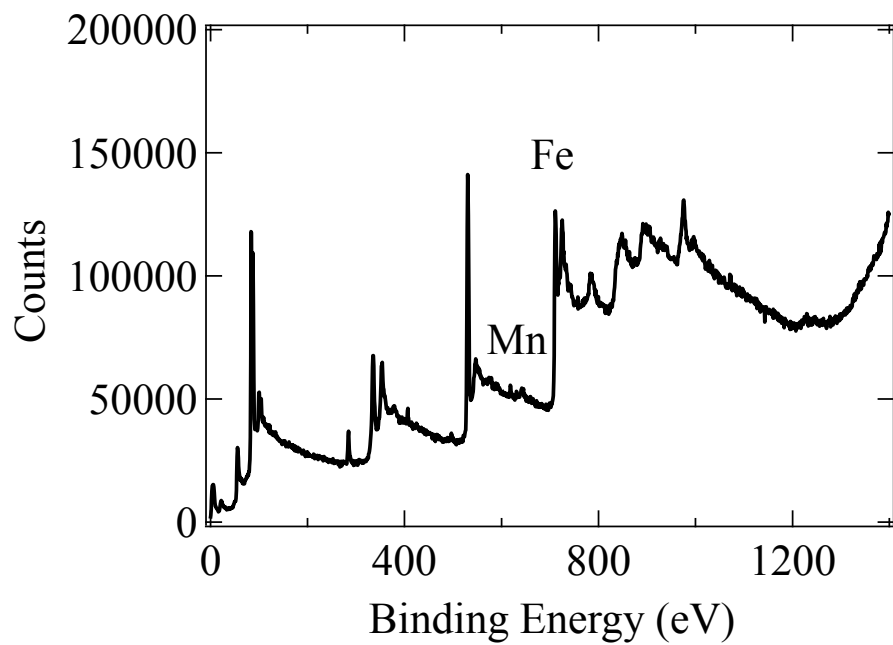
Particles on Corundum



68

69 **Figure S1.** Lorentz-corrected intensity curves of GISAXS scattering caused by ferrihydrite

70 nanoparticles precipitated/deposited on quartz (Figures A1-A3) and corundum (Figures B1-B3)



71

72 **Figure S2.** XPS measurements of ferrihydrite particles formed in FeMn solution

74 **References**

- 75 1. B. L. Henke, E. M. Gullikson and J. C. Davis, *Atomic data and nuclear data tables*, 1993,
76 **54**, 181-342.

77